5th US Combustion Meeting
Organized by the Western States Section of the Combustion Institute
and Hosted by the University of California at San Diego
March 25-28, 2007.

Chemical Kinetics of Ethanol Oxidation

J. Li[1], A. Kazakov[2], M. Chaos[3], and F.L. Dryer[3]

[1]Praxair, Inc.,
Tonawanda, NY 14150, USA

[2]NIST Thermodynamic Research Center,
Boulder, CO 80305, USA

[3] Department of Mechanical and Aerospace Engineering, Princeton University,
Princeton, NJ 08544, USA

Experimental profiles of stable species mole fractions are reported for ethanol oxidation in a Variable Pressure Flow Reactor (VPFR) at initial temperatures of 800-950K, constant pressures of 3 to 12atm, and equivalence ratios from 0.3 to 1.4. A detailed mechanism for ethanol combustion is developed in a hierarchical manner. Each kinetic subset comprising the present mechanism was tested by thorough comparison of model predictions and experimental results found in laminar premixed flames, shock tubes, and flow reactors [Li, PhD thesis (2004); Li et al. *International Journal of Chemical Kinetics* 39 (2007) 109-136]. In this study, the assembled mechanism is further tested against the ethanol oxidation data collected in the VPFR as well as shock-tube ignition data, laminar burning velocities, and structures of counterflow diffusion and partially premixed flame available in the literature. The present ethanol mechanism performs well against this wide ranging set of data and shows a significant improvement of predictions of the newly collected VPFR data over results obtained using other recently published mechanisms [N.M. Marinov, *International Journal of Chemical Kinetics* 31 (1999) 183-220; P. Saxena, F.A. Williams, *Proceedings of the Combustion Institute* 31 (2007) 1149-1156].

1. Introduction

Ethanol (C_2H_5OH) is a very important energy carrier that can be produced from renewable energy resources. It can be used as a fuel extender, octane enhancer, and oxygen-additive in, or as an alternative, neat fuel to replace reformulated gasoline. Ethanol also has potential as a hydrogen carrier for fuel cell applications. The 1990 Clean Air Act Amendments [1] presently require the addition of oxygenates to reformulated gasoline, with seasonal adjustments, on the premise that oxygen content decreases automotive emissions, particularly smog generation participants and carbon monoxide. Ethanol is favored to replace methyl tertiary butyl ether (MTBE), another widely used oxygenate additive that has become unpopular based upon ground water contamination and human health effects. While most ethanol is currently generated by fermentation (grain alcohol), recent developments suggest that ethanol fuel can be derived more efficiently from other biomass, thus offering potential to reduce dependence on fossil fuel energy resources.

The chemistry of gas-phase oxidation and pyrolysis of ethanol have been the subjects of numerous studies over the last five decades. Data have been reported from shock tubes, static

reactors, flow reactors, diffusion flames, and laminar premixed flame experiments. Norton and Dryer [2] conducted a series of ethanol oxidation experiments in an Atmospheric Pressure Flow Reactor (APFR). In the modeling efforts of Norton and Dryer, as well as those of several other investigators [3-5] the importance of including all three isomeric forms of C_2H_5O produced by H-atom abstraction from ethanol was emphasized. Marinov [6] carried out an extensive detailed kinetic modeling study of ethanol combustion at intermediate and high temperatures. His computational results indicated that ethanol oxidation exhibits strong sensitivity to branching ratio assignments of the H-atom abstraction reactions of ethanol as well as to the kinetics of its uni-molecular decomposition. The mechanism performed reasonably well under the experimental conditions found in laminar premixed flames, shock tubes, and the APFR. More recently, Saxena and Williams [7] developed an ethanol mechanism by extending prior kinetic efforts on small hydrocarbon chemistry (i.e. their evolving "San Diego Mechanism" [8]). The ethanol subset of reactions added to their earlier work was taken initially from work developed in our laboratory [9, 10], on which the present study is based. Saxena and Williams [7] measured species profiles in counterflow flames and published comparisons of their model against their data as well as published shock tube ignition delay, burning velocity, and extinction measurements, claiming superiority of the predictive nature of their model against their experiments in comparison to that found using the kinetic model developed in [9], and discussed below. However, no model comparisons against pyrolysis and high-pressure oxidation characteristics of ethanol at flow reactor conditions found in [9] were presented, which include data from which new rate determinations for ethanol uni-molecular decomposition reactions were obtained [11, 12].

We noted in earlier publications [9-12] that ethanol uni-molecular decomposition is important (as also observed by Marinov [6]), even under oxidation conditions at temperatures found in the flow reactor as well as other combustion systems. Uncertainties in the uni-molecular decomposition reactions of ethanol, and branching ratio assignments of the H-atom abstraction reactions by H and CH_3 radicals are such that these reactions must be collectively considered if ethanol pyrolysis is to be predicted well. Upon this validation result, the selection of other abstraction reaction channels and branching ratios relevant to oxidative conditions must be considered in light of the parameter combinations used for modeling pyrolysis. We found that the model of Marinov [6] would not predict pyrolysis data [11], principally because of the assigned rates for the uni-molecular decomposition channels and subsequent impact of the selection of abstraction channel parameters and branching ratios. Hence, its predictions of oxidation results were also compromised, as shown below. As a result, we set about developing a new comprehensive pyrolysis and oxidation model and to also develop a broader set of pyrolysis and oxidation flow reactor validation data.

We first studied the uni-molecular decomposition channels of ethanol, deriving new parameters from radical trapping experiments [12], then developed the abstraction reaction parameter and branching sub model components important to predicting pyrolysis experiments. Subsequently, a full model was developed to predict ethanol pyrolysis and oxidation observations. The pyrolysis results have been extensively discussed in the literature previously [11, 12]. The present paper reports in a comprehensive manner new flow reactor data for ethanol oxidation at high-pressure conditions (3-12 atm) with initial temperatures of 800-950K and equivalence ratios ranging from 0.6 to 1.4 and discusses the oxidation model development and performance, detailed in [9] and briefly summarized earlier in [10]. Here we briefly describe the hierarchical development of the present model and compare predictions against a wide range of experimental

data, including the present high-pressure flow reactor results, shock tube ignition delay data, and flame measurements. We also present for the first time predictions using the recent mechanism of Saxena and Williams [7] against our flow reactor oxidation data. These model predictions are inferior to those generated using the present model.

2. Experimental Methods

Experiments were conducted in the Princeton Variable Pressure Flow Reactor (VPFR). A schematic of the flow reactor is shown in Figure 1. Detailed information about the VPFR instrumentation and experimental methodology can be found in other publications [12, 13], and only a brief description of these issues is given here.

Carrier gas (N_2 in this study) is heated by a pair of electrical resistance heaters and directed into a reactor duct. Oxygen is also introduced at the duct entrance. The carrier gas/oxygen mixture flows around a baffle plate into a gap serving as the entrance to a diffuser. The vaporized fuel (ethanol) flows into the center tube of a fuel injector, and injected radially outward into the gap where it rapidly mixes with the carrier gas and oxygen. The reacting mixture exits the diffuser into a constant area test section. Near the exit of the test section, a sampling probe is positioned on the reactor centerline to continuously extract and convectively quench a small portion of the flow. At the same axial location, the local gas temperature is measured with a type R thermocouple accurate to ±3 K.

The sample gas flows via heated Teflon lines to analytical equipment including a Fourier transform infrared spectrometer (FTIR), an electrochemical O_2 analyzer, and a pair of non-dispersive infrared analyzers for CO and CO_2. The majority of the stable species of interest (C_2H_5OH, H_2O, C_2H_4, CH_4, CH_3CHO, etc.) are measured continuously on-line using FTIR spectrometry. The measurement uncertainties for the data reported here are: O_2 - ±2%, CO - ±2%, CO_2 - ±2%, C_2H_5OH - ±3%, H_2O - ±6%, C_2H_4 - ±3%, CH_4 - ±4%, CH_3CHO - ±3%, CH_2O - ±3%, C_2H_6 - ±4%, and C_2H_2 - ±3% of reading. Additional species can be determined using discrete gas samples acquired from the sample flow and off-line gas chromatographic analyses.

The distance between the point of fuel injection and the sampling position is varied by moving the fuel vapor injector probe (with attached mixer/diffuser assembly), relative to the fixed sampling location. Mean axial velocity measurements along the centerline of the reactor are used to correlate distance with residence time. In this way, profiles of stable species versus the residence time can be determined experimentally. The uncertainty in the reported residence times is approximately 5%.

A series of species-time history ethanol oxidation (C_2H_5OH/O_2 in balance N_2) experiments were conducted in the VPFR at initial temperatures of 800-950K, pressures of 3-12 atm, equivalence ratios of 0.6-1.4, and a fixed initial C_2H_5OH molar concentration of 0.3%. In all of the experiments, the total carbon and oxygen balances experimentally determined at each residence time were within 5% of the specified input. The steady total carbon and oxygen concentrations at each sampling location not only provide verification of the experimental measurements, but also imply that any other carbon- or oxygen-containing stable species are present in negligible quantities. This result was also verified by off-line gas chromatographic analyses.

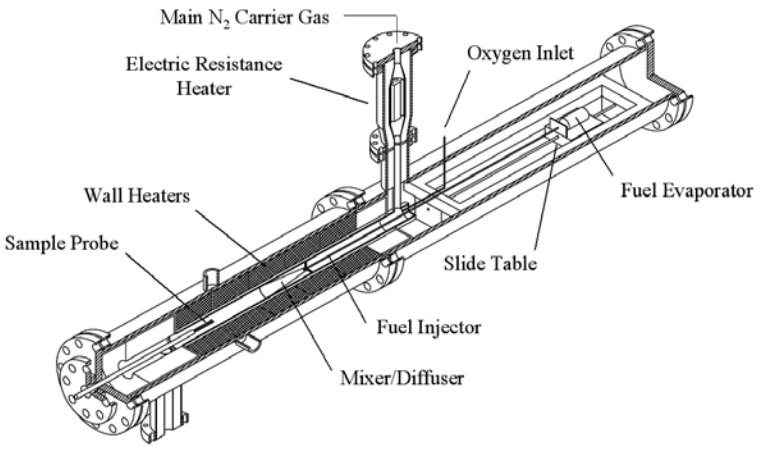

Figure 1: Schematic of the variable pressure flow reactor (VPFR).

3. Chemical Kinetics Model

Predictions using the ethanol mechanisms of Marinov [6] and Saxena and Williams [7] are compared with the present experimental data for two representative cases at 3 and 9 atm in Figs. 2 and 3. The model predictions are compared to the experimental measurements by shifting the simulated values along the time axis to match the 50% fuel consumption point. The predicted fuel and oxygen consumption rates, as well as the production rates of major intermediates, such as H_2O, CH_4, and C_2H_4 are substantially different from the experimental results, independent of any time shifting considerations. Predictions from the model of Saxena and Williams [7] are reasonable for the lower pressure case (Fig. 3a); however they deteriorate as pressure increases (Fig. 3b). In fact, at 9 atm a positive time shift is required to match the experimental 50% fuel consumption location, which is unphysical and usually indicates that the induction time is under predicted by the model even without consideration of mixing effects. Saxena and Williams [7] adopted rate parameters for ethanol decomposition and abstraction reactions directly from [9] (the basis of the present work). This indicates that the source of the discrepancy is not incorrect initiation and branching ratio assignments, shown to be highly coupled in ethanol pyrolysis experiments [11, 12] and points to deficiencies at the lower molecular level.

The detailed pyrolysis and oxidation model reported here consists of 39 species and 238 reversible elementary reactions and was developed in a *comprehensive, hierarchical* manner. The combustion of hydrocarbon species follows a basic series of steps, beginning with initiation decomposition reactions, followed by radical attack on the fuel, production of generally smaller intermediates, and finally a chain of aldehyde $\rightarrow$ CO $\rightarrow$ CO_2 steps. In the above process, the radical pool responsible for chain propagation, branching, and termination is mainly determined by the H_2/O_2 reaction mechanism. By taking these basic steps in the reverse order, the detailed mechanism was built hierarchically. The present ethanol mechanism development initially involved further consideration of the H_2 oxidation sub-mechanism, followed by C_1 sub-mechanism including CO, CH_2O, CH_3OH, and CH_4 combustion, then the C_2 sub-mechanism components including the reactions for C_2H_X (X = 1–6), CH_3CHO, and C_2H_5OH. The hierarchy of the development of the ethanol chemical kinetics model is shown in Fig. 4.

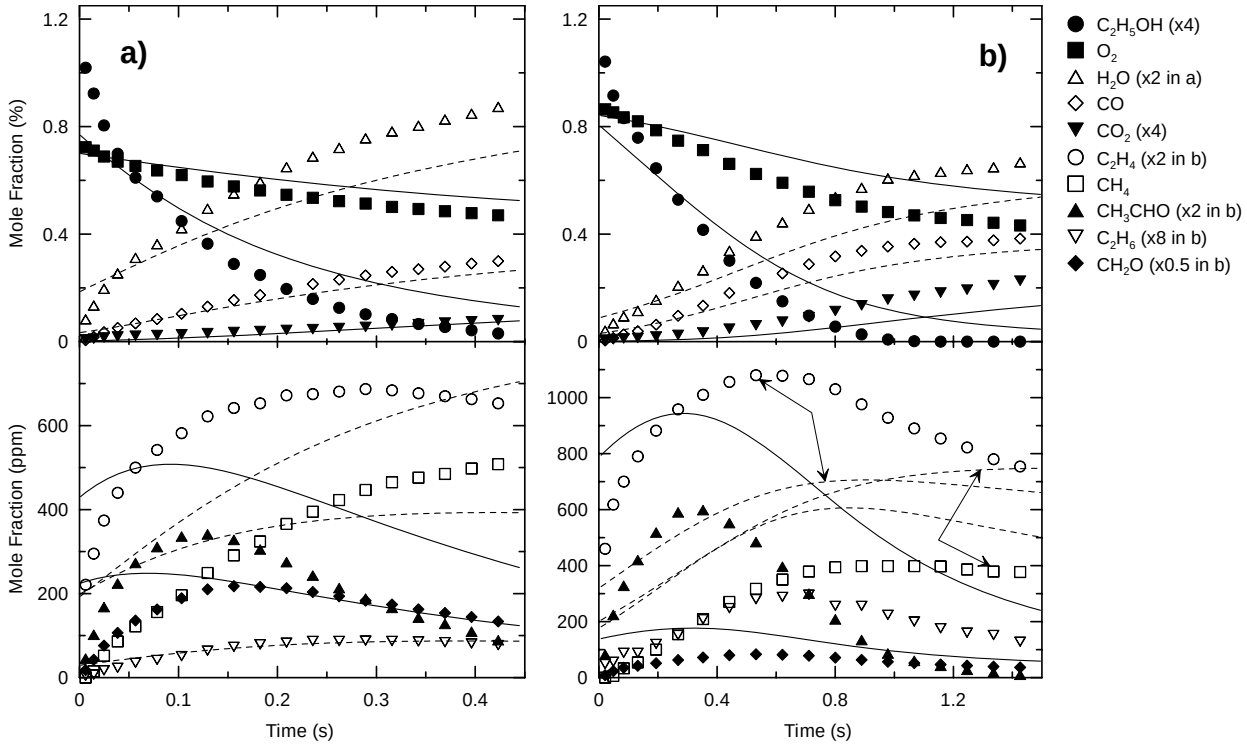

Figure 2: Oxidation of $C_2H_5OH/O_2/N_2$ mixtures in the VPFR. Initial conditions: a) P = 3 atm, T = 950 K, 0.3 % C_2H_5OH concentration, ϕ = 1.2; b) P = 9 atm, T = 830 K, X_{C2H5OH} = 0.3%, ϕ = 1. Symbols are present experimental measurements, lines are modeling predictions using the mechanism of Marinov [6]; dashed lines correspond to open symbols. Predictions have been shifted by –0.17 s (a) and –0.88 s (b).

At each level, the newly added portions of the mechanism were tested and validated by thorough comparison with experimental data over wide ranges of physical conditions for the sub-mechanism species. These experimental sources included laminar flame speeds, shock tube ignition delay data, flow reactor measurements, and other sources such as observations in static and stirred reactors. In conjunction with sensitivity and reaction flux analyses, the selected starting sub-mechanisms (H_2/O_2 mechanism of Mueller et al. [14], CH_3OH/O_2 mechanism of Held and Dryer [15], and C_2H_5OH/O_2 mechanism of Marinov [6]), were updated and/or revised to reflect recent publications of thermodynamic data, rate coefficients, and channel results. Detailed information of each level of the present ethanol mechanism development can be found elsewhere [9, 16]. A brief summary of important considerations is presented below.

H_2/O_2 sub-mechanism. The entire sub-mechanism was replaced with our recent updated version [17] of that published earlier by Mueller et al. [14]. The revised mechanism encompasses recently published thermodynamic data for OH and rate constants for two important reactions: H + O_2 = OH + O [18] and H + O_2 (+M) = HO_2 (+M) [19]. Sensitivity analyses show that the reaction H + OH + M = H_2O + M is of significance to the observations in high-pressure flame propagation. Its rate constant was modified within known uncertainty limits to achieve flame propagation model performance.

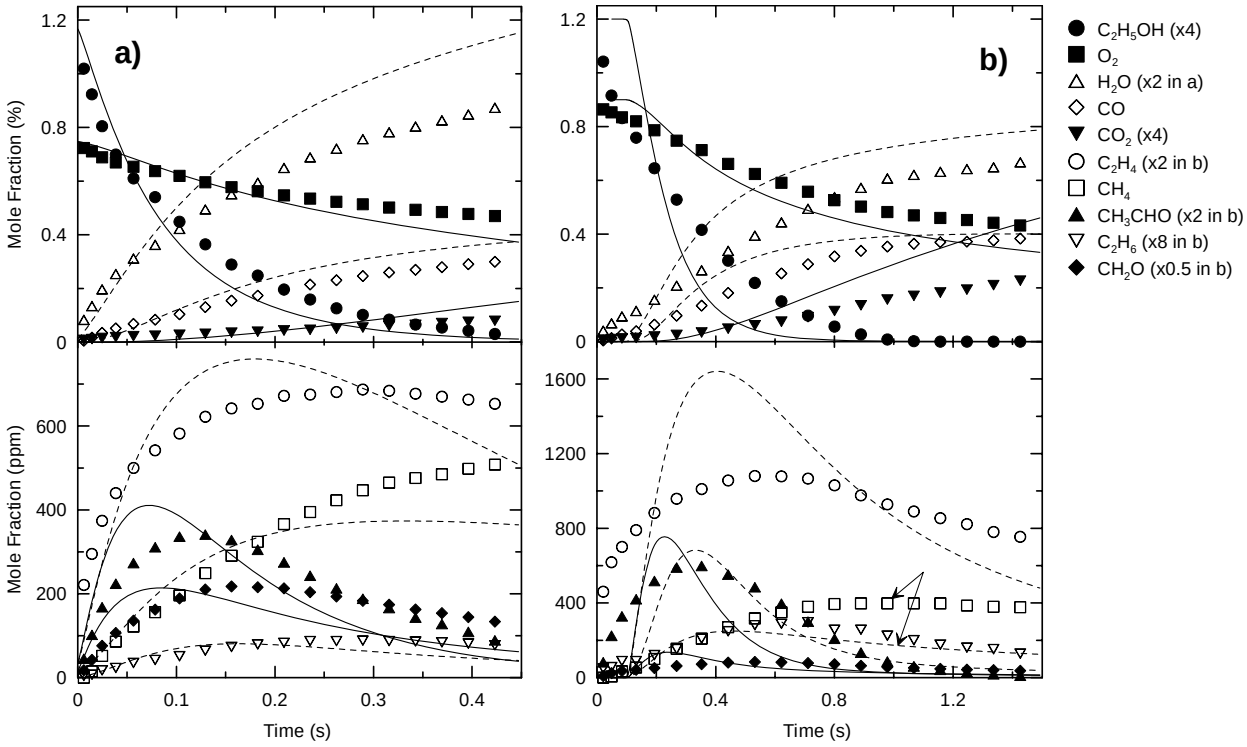

Figure 3: Oxidation of $C_2H_5OH/O_2/N_2$ mixtures in the VPFR. Initial conditions: a) P = 3 atm, T = 950 K, 0.3% C_2H_5OH concentration, ϕ = 1.2; b) P = 9 atm, T = 830 K, X_{C2H5OH} = 0.3 %, ϕ = 1. Symbols are present experimental measurements, lines are modeling predictions using the mechanism of Saxena and Williams [7]; dashed lines correspond to open symbols. Predictions have been shifted by –30 ms (a) and +50 ms (b).

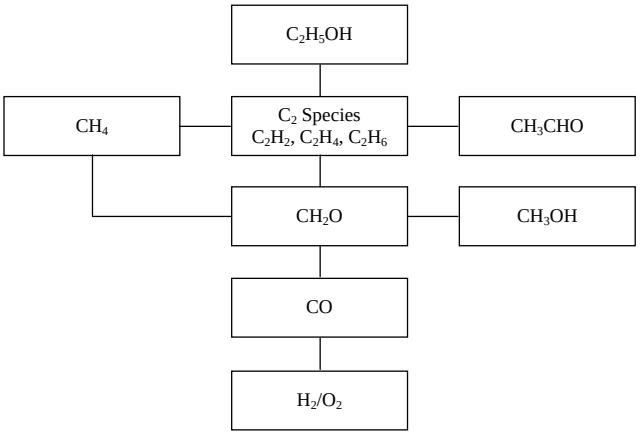

Figure 4: Hierarchical structure of the present ethanol oxidation mechanism.

CO, CH_2O, CH_3OH/O_2 sub-mechanism. The C_1 sub-mechanism was developed based on the CH_3OH/O_2 mechanism of Held and Dryer [15]. Recently, kinetic parameters for CH_3, HCO, and CH_2O related reactions as well as new experimental data for C_1 species have become available. The CO/O_2, CH_2O/O_2, and CH_3OH/O_2 mechanisms were revisited, considering the new kinetic information. The most important revisions to the original model involve the rate constant

descriptions for the reactions CO + OH = CO_2 + H and HCO + M = H + CO + M. Recent theoretical calculations of the rate constant of CO + OH = CO_2 + H predict values higher than experimental measurements at low to intermediate temperatures [16]. The temperature-dependent sensitivity analysis of Zhao et al. [20] demonstrates that flame speeds of hydrocarbons are most sensitive to the value of the rate constant of HCO + M = H + CO + M at 1300–2000K, well above the range of conditions of the recently published measurement for this reaction. After an exhaustive literature review, Li et al. [16] performed weighted least square fits on the entire body of experimentally measured rate constants for these two reactions yielding the following expressions:

$$k_{\mathrm{CO+OH=CO_2+H}} = 2.23\times10^{5} T^{1.89} \exp\left(\frac{583}{T}\right) \qquad k_{\mathrm{HCO+M=H+CO+M}} = 4.75\times10^{11} T^{0.66} \exp\left(-\frac{7485}{T}\right)$$

Further description of the C_1 sub-mechanism, including its validation against a wide range of experimental data can be found in Ref. 16. Since the initial development of the mechanism, recent works [21-23] suggest that the reaction parameters for the reaction CO+HO_2=CO_2+H are substantially less than originally recommended by Mueller et al. [14]. More detailed discussions pertaining to this issue appear in Ref. 16. The substitution of these new rate parameters into the C_1 sub-mechanism have no significant effect on any of the predictions reported here.

C_2H_X /O_2 sub-mechanism. The C_2H_X (X = 1–6), as well as CH_2 and HCCO sub-models were primarily taken from the C_2 chemistry of Wang et al. [24], which was derived from the GRI-1.2 mechanism [25]. Wang et al. [24] tested their mechanism against a variety of C_2H_2 and C_2H_4 experiments, including ignition behavior, laminar flame propagation, and detailed structure of burner-stabilized flames, and the mechanism was demonstrated to reproduce most of the experiment results.

CH_3CHO/O_2 sub-mechanism. Acetaldehyde combustion chemistry, including CH_3CHO, CH_3CO, CH_2CHO, and CH_2CO reactions, was based on the sub-mechanism appearing in Marinov [6]. All acetaldehyde mechanisms currently available in literature (e.g. [6, 26, 27]) failed to give reasonable predictions of acetaldehyde experiments previously conducted in the VPFR [28]. The discrepancy makes clear that considerable work remains to reconcile predictions with experimental measurements. Here we made revisions to elementary acetaldehyde reactions based on an extensive literature review, especially for decomposition as well as abstraction reactions involving OH. Further studies on the acetaldehyde decomposition and abstraction reactions with other radicals, like HO_2, are continuing.

C_2H_5OH/O_2 sub-mechanism. The ethanol subset consists of ethanol decomposition reactions, abstraction reactions generating three isomeric forms of C_2H_5O due to the three possible sites for H-atom abstraction in C_2H_5OH molecules, and subsequent reactions of C_2H_5O to produce C_1 or other C_2 species whose mechanism has been established above. The current ethanol sub-mechanism was based on that of Marinov [6] with revisions to ethanol decomposition and abstraction reactions. The fall-off kinetics of ethanol decomposition was described by our recent study based on pyrolysis experiments [11] with radical trappers and RRKM/master equation calculations [12]. Extensive literature review of ethanol abstraction reactions shows there are very few elementary experimental measurements available. In the present study, the rate constants of abstraction reactions were modified to better reproduce the VPFR experiments [9].

Thermodynamic data. The thermodynamic properties of species found in the detailed mechanism were primarily obtained from the CHEMKIN thermodynamic database [29] and Burcat's thermochemical database [30], except for OH, HO_2, and CH_2OH. The standard heats of formation of OH and HO_2 at 298 K were updated to 8.9 kcal/mol [31] and 3.0 kcal/mol [32], respectively. Recently, Ruscic et al. [33] have updated the heat of formation for HO_2 to 2.94± 0.06 kcal/mol. This change makes no significant difference in the quality of predictions obtained in the present work, for our laboratory has consistently used a heat of formation for HO_2 within the uncertainties of the now accepted value in all of our previous modeling studies. The thermochemical properties of CH_2OH, including enthalpy of formation, standard entropy, and heat capacity at different temperatures, were taken from [34] and agree with the recent evaluation of Ruscic et al. [35].

4. Results and discussion

The ethanol mechanism described above was compared against the expansive set of VPFR experiments performed in this study. The combined results are shown in Figs. 5-8. The predictions of the major stable species (C_2H_5OH, O_2, H_2O, CO, and CO_2) using the present mechanism agree very well with the experimental measurements and represent a significant improvement over predictions using the mechanisms of Marinov [6] and Saxena and Williams [7] (see Figs. 2 and 3). For other stable species, the model predictions are reasonable but can be further improved, especially at higher pressures. Mechanistic elements, particularly those involving acetaldehyde and its reactive intermediates, remain under consideration in further improving the present version of the ethanol oxidation mechanism. The quality of predictions of the present mechanism for the atmospheric pressure flow reactor data of Norton and Dryer [2] is similar to that shown in Figs. 5-8. Clearly ethanol pyrolysis calculations are also in very good agreement with the experiments of Li et al. [11] as the uni-molecular decomposition rates used in the present mechanism were adopted from that study.

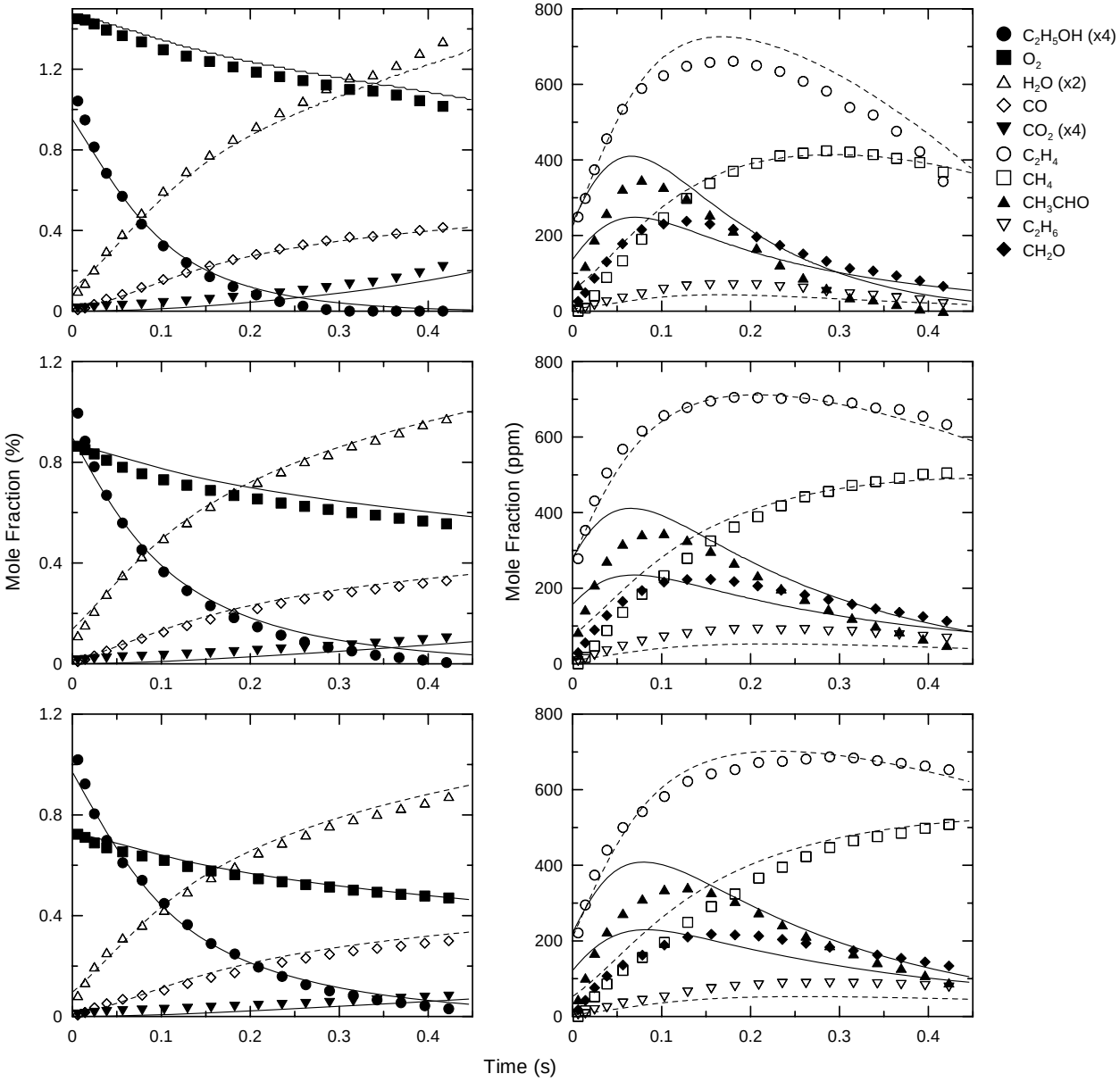

Figure 5: Time evolution of stable major (left) and minor intermediate (right) species during VPFR oxidation of $C_2H_5OH/O_2/N_2$ mixtures at 3 atm, initial temperature of 950 K, and initial molar fuel concentration of 0.3 %: top – ϕ = 0.6; middle – ϕ = 1.0; bottom – ϕ = 1.2. Symbols are experimental measurements; lines are predictions from the present model. Dashed lines correspond to open symbols. Computed profiles have been shifted by –98 ms (top), –110 ms (middle), and –106 ms (bottom).

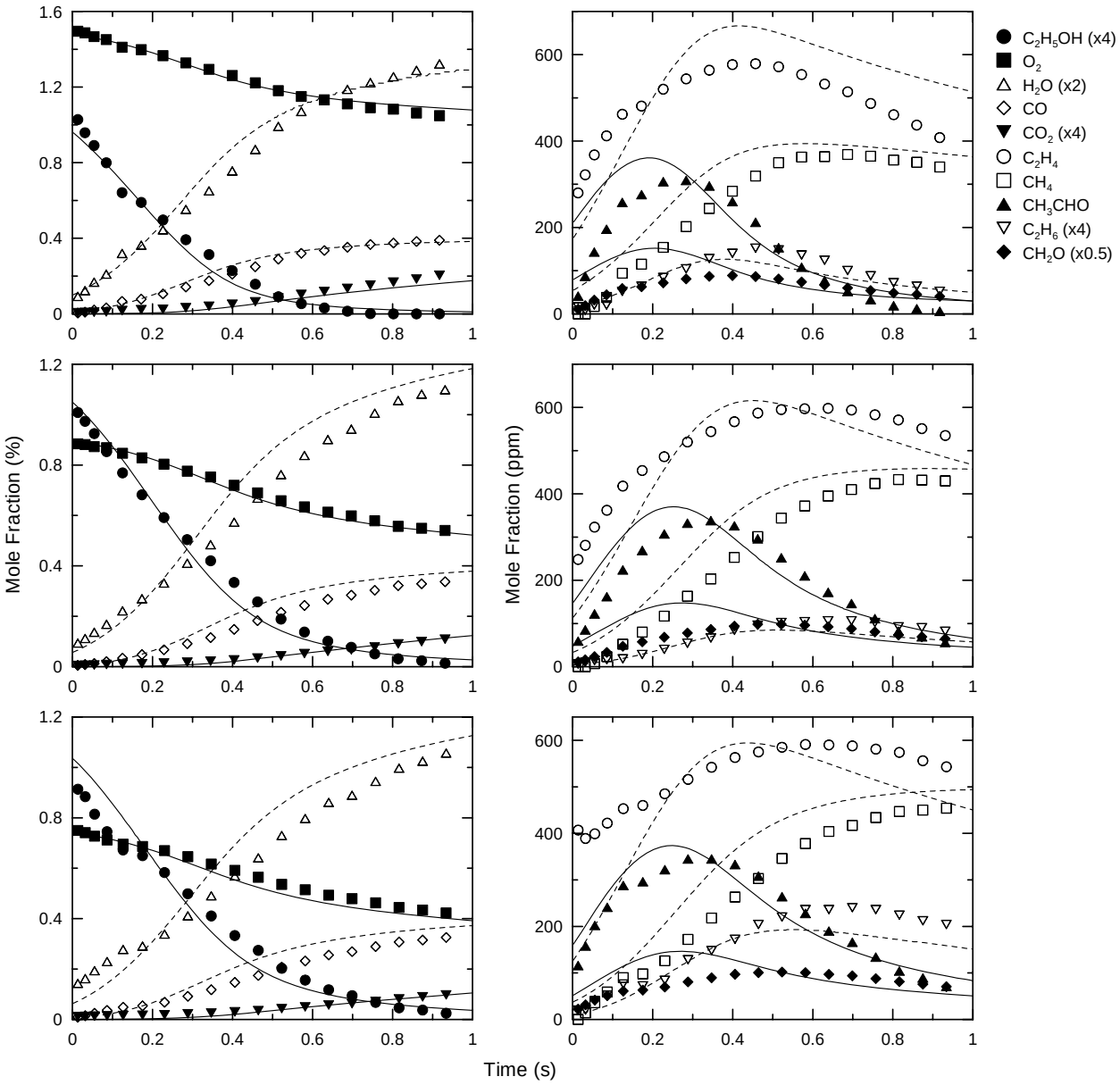

Figure 6: Time evolution of stable major (left) and minor intermediate (right) species during VPFR oxidation of $C_2H_5OH/O_2/N_2$ mixtures at 6 atm, initial temperature of 860 K, and initial molar fuel concentration of 0.3 %: top – ϕ = 0.6; middle – ϕ = 1.0; bottom – ϕ = 1.2. Symbols are experimental measurements; lines are predictions from the present model. Dashed lines correspond to open symbols. Computed profiles have been shifted by –0.40 s (top), –0.35 s (middle), and –0.35 s (bottom).

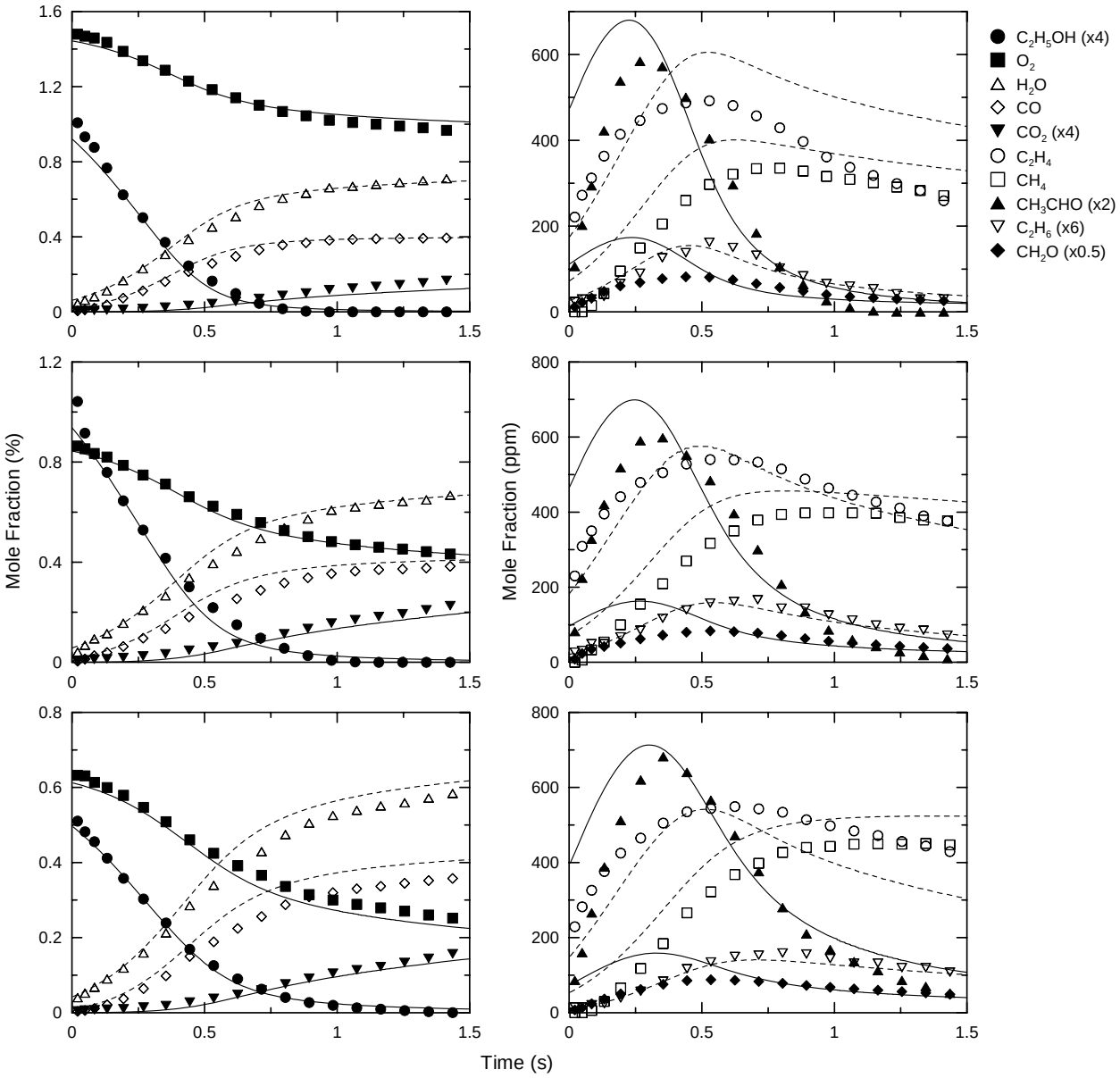

Figure 7: Time evolution of stable major (left) and minor intermediate (right) species during VPFR oxidation of $C_2H_5OH/O_2/N_2$ mixtures at 9 atm, initial temperature of 830 K, and initial molar fuel concentration of 0.3 %: top – ϕ = 0.6; middle – ϕ = 1.0; bottom – ϕ = 1.4. Symbols are experimental measurements; lines are predictions from the present model. Dashed lines correspond to open symbols. Computed profiles have been shifted by –0.66 s (top), –0.65 s (middle), and –0.60 s (bottom).

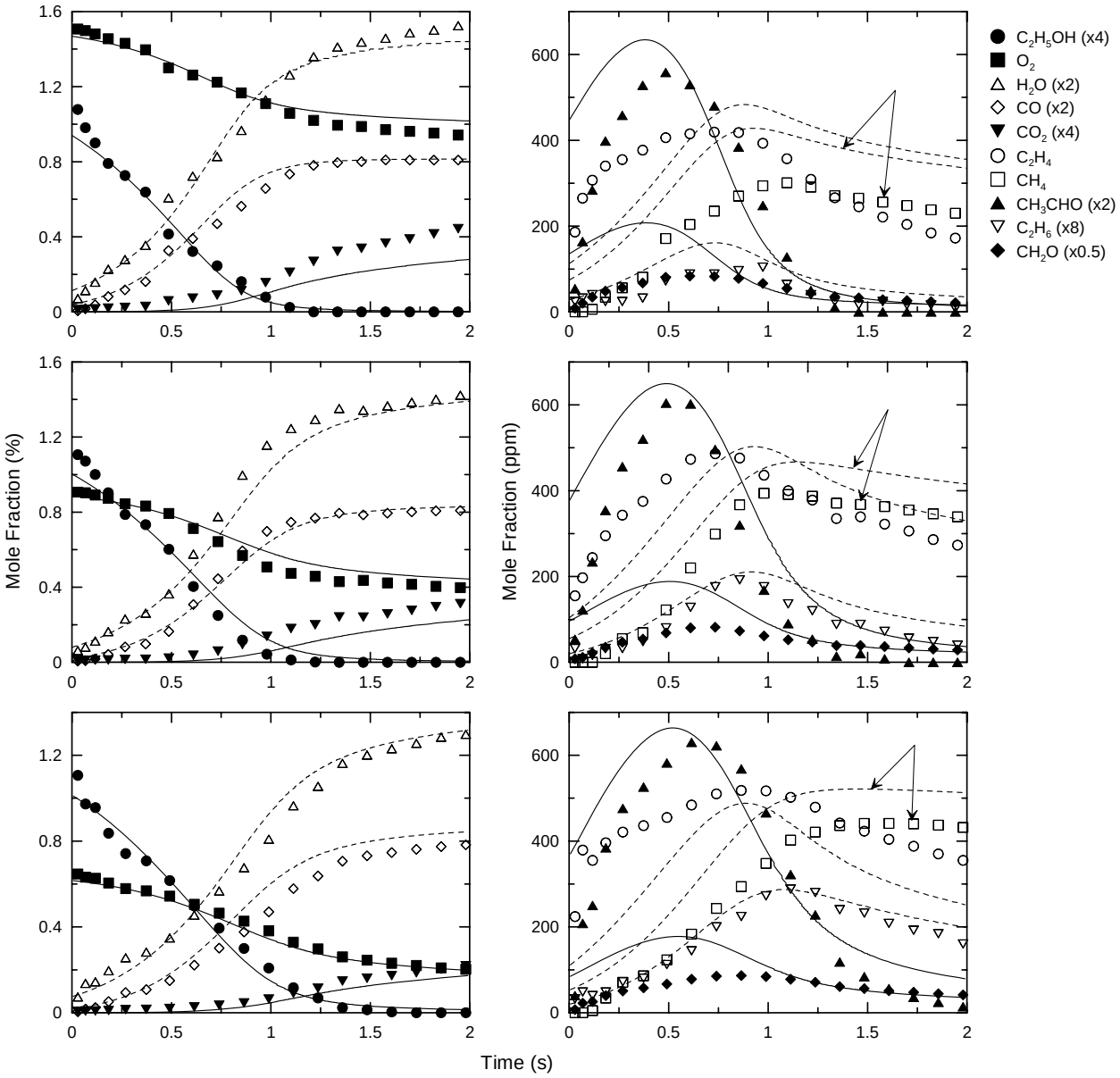

Figure 8: Time evolution of stable major (left) and minor intermediate (right) species during VPFR oxidation of $C_2H_5OH/O_2/N_2$ mixtures at 12 atm, initial temperature of 800 K, and initial molar fuel concentration of 0.3 %: top – ϕ = 0.6; middle – ϕ = 1.0; bottom – ϕ = 1.4. Symbols are experimental measurements; lines are predictions from the present model. Dashed lines correspond to open symbols. Computed profiles have been shifted by –1.20 s (top), –1.10 s (middle), and –1.08 s (bottom).

The present ethanol mechanism was also tested against experimental observations found in shock tubes, laminar premixed flames, and counterflow flames. The SENKIN [36], PREMIX [37], and OPPDIF [38] codes were used for ignition delay, laminar burning velocity, and counterflow flame calculations, respectively. The standard CHEMKIN transport package was used for the counterflow as well as burning velocity calculations with Soret effects and multi-component diffusion included. The resolution of imposed grids was such that fully converged solutions were obtained for both PREMIX and OPPDIF calculations.

Ignition of $C_2H_5OH/O_2/Ar$ mixtures has been studied behind reflected shock waves by Natajaran and Bhaskaran [3], Dunphy et al [4, 5], and Curran et al. [39]. Experiments spanned temperatures of 1100 to 1700 K, pressures of 1 to 4.5 atm, and equivalence ratios of 0.25 to 2.0. Figure 9 presents results of calculated ignition delays using the present mechanism compared against the data of Natajaran and Bhaskaran [3] and Curran et al. [39]; reasonable agreement is shown. The model captures the experimentally observed insensitivity of ignition delay to changes in stoichiometry (Fig. 9a). For the higher pressure experiments of Curran et al. [39], the model predictions exhibit a similar pressure dependence as that seen experimentally but overpredict the overall activation energy (Fig 9b).

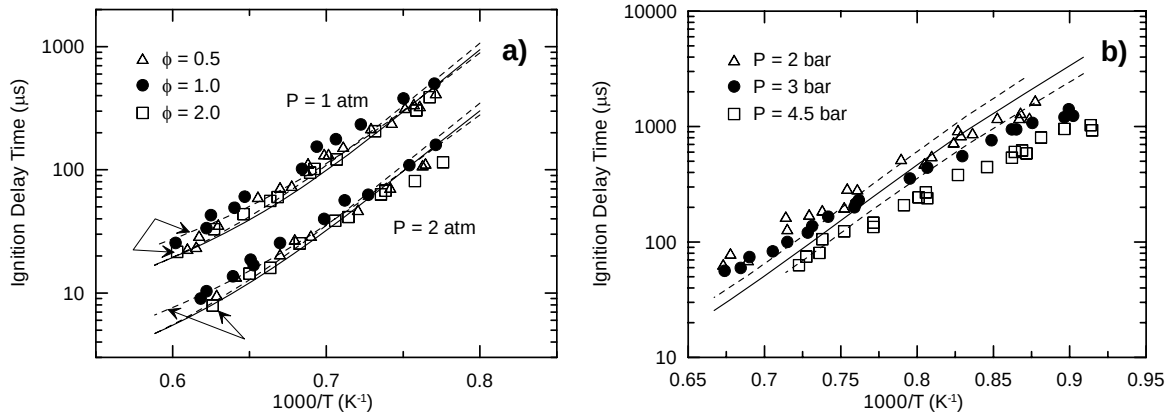

Figure 9: Ignition delays of $C_2H_5OH/O_2/Ar$ mixtures in a shock tube. a) Model comparisons against data of Natajaran and Bhaskaran [3] at 1.43% (ϕ = 0.5), 2.5% (ϕ = 1.0), and 4.0% (ϕ = 2.0) initial C_2H_5OH molar concentration. Results for P = 2 atm have been reduced by half for clarity; b) Model comparisons against data of Curran et al [39] at stoichiometric conditions and an initial molar fuel concentration of 2.5%. Symbols are experimental data with lines showing prediction using the present model. Dashed lines correspond to open symbols.

Figure 10 compares predicted laminar burning velocities against the measurements of Gülder [40] and Egolfopoulos et al. [41]. The measurements were performed in different experimental devices (i.e. a spherical bomb [40] and counterflow burner [41]) at pressures up to 8 atm [41] and initial temperatures up to 453 K [41]. Good agreement is observed in Fig. 10 for atmospheric flames at all temperatures considered. The model also predicts well the burning velocity at elevated pressures.

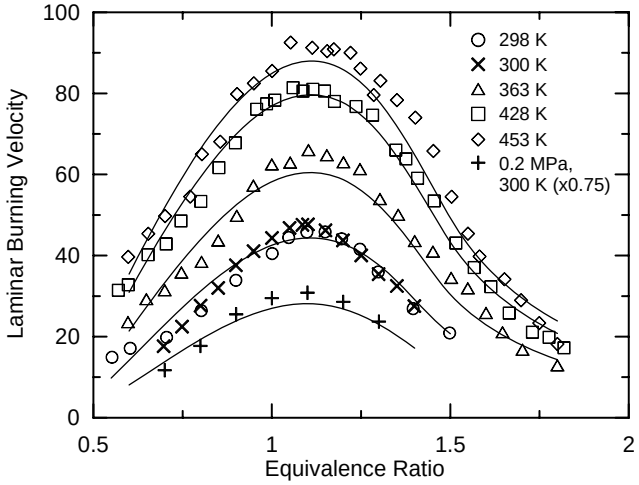

Figure 10: Laminar burning velocities of ethanol/air mixtures. Open symbols correspond to the measurements of Egolfopoulos et al. [41] at atmospheric pressure; other symbols are the measurements of Gülder [40]. Lines are predictions of the present model.

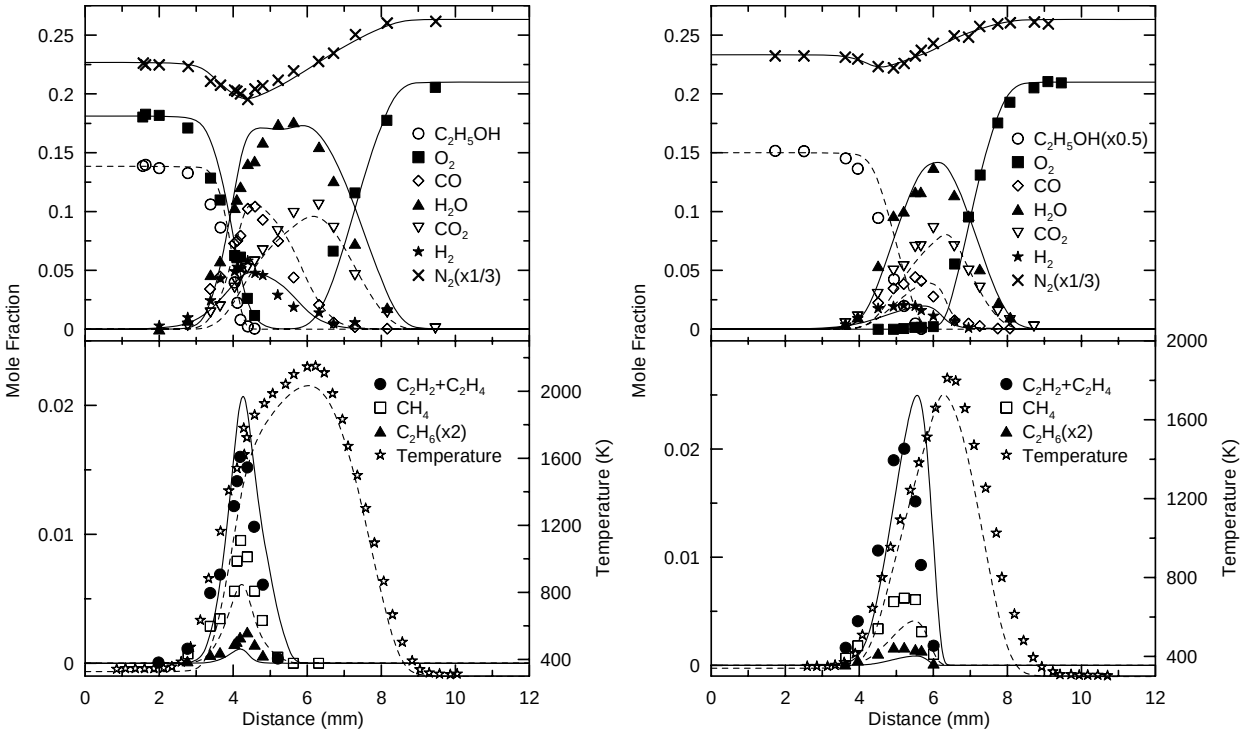

Figure11: Species and temperature profiles of ethanol partially premixed (left) and diffusion (right) counterflow flames. Symbols are measurements of Saxena and Williams [7], lines are present model predictions. Dashed lines correspond to open symbols.

Saxena and Williams [7] performed experiments on flame structures using a counterflow burner. Measurements were performed on both partially premixed and diffusion systems at a strain rate of 100 s^{-1}. The study of Saxena and Williams [7] has recently appeared in the open literature and the measurements reported present an opportunity to test present model predictions against new

data not utilized in its development. Figure 11 shows the results of the flame measurements [7] against calculations using the present mechanism. Very good agreement can be observed for the major species. There is a slight overprediction of the combined concentration of ethylene and acetylene and both methane and ethane are underpredicted by nearly 35% and 50% respectively. The quality of predictions from the present mechanism is comparable to that obtained by Saxena and Williams [7] using their model except for methane which was better predicted. This result can be explained by the lower rate chosen in [7] for methyl radical recombination relative to that used in the present model, which leads to higher methane production by the channeling of methyl radicals through CH_3+H recombination. In the present mechanism the latest update to the $CH_3+CH_3=C_2H_6$ reaction is used [43] and it is noted that Saxena and Williams [7] employ a dated value [44]. Nonetheless, increasing the rate of H abstraction by methyl from ethanol by a factor of 2 would bring methane predictions within experimental uncertainty whereas only altering flow reactor methane profiles (Fig. 5-8) by 15%. As discussed by Saxena and Williams [7] the discrepancy between measured and predicted ethane profiles may be removed by decreasing the rate of the reaction $C_2H_6+H = C_2H_5+H_2$. It is not our intent in this paper to modify the model described here to better predict the new flame data [7]. To perfom such a task would require the re-validation of the model not only for ethanol targets presented here but also for targets used in its development at the lower molecular subsets.

5. Conclusion

Species evolution profiles during the high pressure oxidation of ethanol in a flow reactor have been measured and reported here. Predictions of the new experimental data based upon a previous [6] and a recently published ethanol oxidation mechanism [7] are significantly deficient. The new comprehensive detailed kinetic model developed herein takes advantage of the hierarchal nature of reacting systems, beginning with the H_2/O_2 reaction mechanism [17], and subsequently encompassing C_1/O_2 (thoroughly updated and tested by Li et al. [16]), C_2H_X/O_2, CH_3CHO/O_2, and C_2H_5OH/O_2 subsets in order of increasing complexity. The relevant mechanism consists of 39 species and 238 reactions. Important updates/modifications to the original ethanol reaction subset (based on the work of Marinov [6]) were made to reflect recent updates of thermodynamic data, rate coefficients, and branching ratios. The present mechanism has been validated by thorough comparison between numerically predicted and experimentally observed results found in laminar premixed flames, shock tubes, counterflow flames, and flow reactors including the experiments reported herein. Predictions are reasonably good for the major species profiles observed in the new VPFR experiments, and significantly improve the agreement with the experimental targets originally investigated by Marinov [6]. No effort has been made to further minimize the dimensional characteristics of the model for predicting specific validation targets. The present study further demonstrates the continual need to re-evaluate any “comprehensive” mechanism [42] as new experimental validation constraints are considered and/or as improved kinetic and thermochemical parameters become available.

Acknowledgments

This work was supported by the Chemical Sciences, Geosciences and Biosciences Division, Office of Basic Energy Sciences, Office of Science, U.S. Department of Energy under Grant No.

DE-FG02-86ER13503. The authors also thank Mr. Paul Michniewicz for his assistance in performing the experiments.

References

1. Energy Information Administration, Alternatives to Traditional Transportation Fuels (1996) DOE/EIA-0585.
2. T.S. Norton, F.L. Dryer, *International Journal of Chemical Kinetics* 24 (1992) 319-344.
3. K. Natarajan, K.A. Bhaskaran, *Thirteenth International Symposium on Shock Waves* (1981) 834-842.
4. M.P. Dunphy, J.M. Simmie, *Journal of the Chemical Society, Faraday Transactions* 87 (1991) 1691-1696.
5. M.P. Dunphy, P.M. Patterson, J.M. Simmie, *Journal of the Chemical Society, Faraday Transactions* 87 (1991) 2549-2560.
6. N.M. Marinov, *International Journal of Chemical Kinetics* 31 (1999) 183-220.
7. P. Saxena, F.A. Williams, *Proceedings of the Combustion Institute* 31 (2007) 1149-1156.
8. http://www-mae.ucsd.edu/~combustion/cermech/
9. J. Li, PhD thesis, Department of Mechanical and Aerospace Engineering, Princeton University, Princeton, NJ (2004).
10. J. Li, A. Kazakov, F.L. Dryer, European Combustion Meeting, Louvain-la-Neuve, Belgium (2005) Paper 019.
11. J. Li, A. Kazakov, F.L. Dryer, *International Journal of Chemical Kinetics* 133 (2001) 859-867.
12. J. Li, A. Kazakov, F.L. Dryer, *Journal of Physical Chemistry A* 108(2004) 7671-7680.
13. T.J. Held, Ph.D. thesis, Department of Mechanical and Aerospace Engineering, Princeton University, Princeton, NJ, 1993.
14. M.A. Mueller, T.J. Kim, R.A. Yetter, F.L. Dryer, *International Journal of Chemical Kinetics* 31 (1999) 113-125.
15. T.J. Held, F.L. Dryer, *International Journal of Chemical Kinetics* 30 (1998) 805-830.
16. J. Li, Z. Zhao, A. Kazakov, M. Chaos, F.L. Dryer, J.J. Scire, *International Journal of Chemical Kinetics* 39 (2007) 109-136.
17. J. Li, Z. Zhao, A. Kazakov, F.L. Dryer, *International Journal of Chemical Kinetics* 36 (2004) 566-575.
18. J.P. Hessler, *Journal of Physical Chemistry A* 102 (1998) 4517-4526.
19. J.V. Michael, M.C. Su, J.W. Sutherland, J.J. Carroll, A.F. Wagner, *Journal of Physical Chemistry A* 106 (2002) 5297-5313.
20. Z. Zhao, J. Li, A. Kazakov, F.L. Dryer, *International Journal of Chemical Kinetics* 37 (2004) 282-295.
21. G. Mittal, C.J. Sung, M. Fairweather, A.S. Tomlin, J.F. Griffiths and K.J. Hughes, *Proceedings of the Combustion Institute* 31 (2007) 419-427.
22. R. Sivaramakrishnan, A. Comandini, R.S. Tranter, K. Brezinsky, S.G. Davis and H. Wang, *Proceedings of the Combustion Institute* 31 (2007) 429-437.
23. H. Sun, S.I. Yang, G. Jomaas and C.K. Law, *Proceedings of the Combustion Institute* 31 (2007) 439-446.
24. H. Wang, A. Laskin, Z.M. Djurisic, C.K. Law, S.G. Davis, D.L. Zhu, Fall Technical Meeting of the Eastern States Section of the Combustion Institute, Raleigh, NC, pp. 129-132 (1999).
25. M. Frenklach, H. Wang, M. Goldenberg, G.P. Smith, D.M. Golden, C.T. Bowman, R.K. Hanson, W.C. Gardiner, V. Lissianski, GRI Technical Report No. GRI-95/0058 (1995).
26. A.A. Borisov, V.M. Zamanskii, A.A. Konnov, V.V. Lisyanskii, S.A. Rusakov, G.I. Skachkov, *Soviet Journal of Chemical Physics* 4 (1989) 2561-2537.
27. P. Dagaut, M. Reuillon, D. Voisin, M. Cathonnet, M. McGuinness, J.M. Simmie, *Combustion Science and Technology* 107 (1995) 301-316.
28. D.C Zarubiak, M.S.E. Thesis, Department of Mechanical and Aerospace Engineering, Princeton University, Princeton, NJ (1997).
29. R.J. Kee, F.M. Rupley, J.A. Miller, Sandia National Laboratories Report No. SAND87-8215 (1987).
30. ftp://ftp.technion.ac.il/pub/supported/aetdd/thermodynamics (2007).
31. B. Ruscic, A.F. Wagner, L.B. Harding, R.L. Asher, D. Feller, D.A. Dixon, K.A. Peterson, Y. Song, X. Qian, C. Ng, J. Liu, W. Chen, D.W. Schwenke, *Journal of Physical Chemistry A* 106 (2002) 2727-2747.
32. A.J. Hills, C.J. Howard, *Journal of Chemical Physics* 81 (1984) 4458-4465.
33. B. Ruscic, R.E. Pinzon, M.L. Morton, N.K. Srinivasan, M.-C Su, J.W. Sutherland, J.V. Michael, *Journal of Physical Chemistry A* 110 (2006) 6592-6601.
34. R.D. Johnson III, J.W. Hudgens, *Journal of Physical Chemistry* 100 (1996) 19874-19890.

35. B. Ruscic, J.E. Boggs, A. Burcat, A.G. Csaszar, J. Demaison, R. Janoschek, J.M.L. Martin, M.L. Morton, M.J. Rossi, J.F. Stanton, P.G. Szalay, P.R. Westmoreland, F. Zabel, T. Berces, *Journal of Physical and Chemical Reference Data* 34 (2005) 573-656.
36. A.E. Lutz, R.J. Kee, J.A. Miller, Technical Report SAND87-8248, Sandia National Laboratories (1987).
37. R.J. Kee, J.F. Grcar, M.D. Smooke, J.A. Miller, Technical Report SAND85-8240, Sandia National Laboratories (1985).
38. A.E. Lutz, R.J. Kee, J.F. Grcar, F.M. Rupley, Technical Report SAND96-8243, Sandia National Laboratories (1996).
39. H.J. Curran, M.P Dunphy, J.M. Simmie, C.K. Westbrook, W.J. Pitz, *Proceedings of the Combustion Institute* 24 (1992) 769-776.
40. O.L. Gülder, *Proceedings of the Combustion Institute* 19 (1982) 275-281.
41. F.N. Egolfopoulos, D.X. Du, C.K. Law, *Proceedings of the Combustion Institute* 24 (1992) 833-841.
42. C.K. Westbrook, F.L. Dryer, *Combustion Science and Technology* 20 (1979) 125-140.
43. B. Wang, H. Hou, L.M. Yoder, J.T. Muckerman, C. Fockenberg, *Journal of Physical Chemistry A* 107 (2003) 11414-11426.
44. J.C. Hewson, F.A. Williams, *Combustion and Flame* 117 (1999) 441-476.